SPACE TELESCOPE SCIENCE INSTITUTE
Operated for NASA by AURA

WFC3 Instrument Science Report 2013-02

WFC3 Cycle 19 Proposal 12690: UVIS Gain

H. Gunning, C. Pavlovsky, S. Baggett
Space Telescope Science Institute
January 23, 2013

ABSTRACT

This report summarizes gain calculation results from the Cycle 19 UVIS Gain monitoring proposal 12690 and compares results to previous measurements from Cycle 18, Cycle 17, SMOV (after launch), and TV3 (before launch). Gain values for each quadrant were measured using internal calibration flat field data at the nominal gain setting (1.5 e-/DN) in both binned and unbinned modes. The gain for the unbinned mode was measured to be 1.56, 1.56, 1.58, and 1.57 e-/DN, with errors ∼0.01 e-/DN, for quadrants A, B, C, and D, respectively. These values are within 1-2% of previous values from TV3 through Cycle 18. The Cycle 19 gain measurements for the binned modes are within 1% of the TV3 values; namely, 1.56, 1.56, 1.57, and 1.56 e-/DN for the 2x2 mode and 1.55, 1.54, 1.56, and 1.56 for the 3x3 mode for A, B, C, and D, respectively, with errors ∼0.01 e-/DN.

1 Introduction

The WFC3 UVIS channel CCDs are 2051x4096 silicon-based detectors with 15x15 μm square pixels assembled into a 2x1 mosaic (Dressel, 2012). Each pixel on the CCDs accumulates charge in proportion to the number of photons that strike the pixel. This collected charge is dependent upon how many electrons are excited by a photon hitting the detector. The gain is the measurement of how many electrons are required to register as a digital unit (count) on the CCD. Gain monitoring is essential as it serves as a good proxy for any changes developing in the camera. To track the gain, without using external observing time, we take our measurements with internal flat fields using the calibration tungsten lamps. This report summarizes our data, method, and results for Cycle 19 and compares them to previous measurements.

2 Data

The data for Proposal 12690 (PI: C. Pavlovsky) consists of eight full frame internal flat fields through the F645N filter using the default tungsten lamp. The internal flat fields are obtained using the calibration subsystem (Baggett, 2008). Mounted on the WFC3 optical bench, the subsystem houses the calibration lamp assembly for both the UVIS and IR channels as well as the additional optics necessary to guide the beam onto the detectors. For UVIS internal flatfields, a beamsplitter within the subsystem directs light from the desired bulb onto a sequence of mirrors which send the beam through a hole in the UVIS corrector mirror, through the specified filter and onto the detector. The WFC3 Instrument Handbook, Figure 2.1, provides a schematic of the optical path (Dressel, 2012).

The flat fields were taken with a range of exposure times to achieve levels between ∼500-50,000 e-. Ten orbits were allotted for unbinned data and three were used to test the binned modes. Exposures were spread across several visits and the order of exposures was mixed to reduce systematics. We utilized the optional APT parameter "SEQ NON-INT" for each visit, meaning our data were taken back-to-back without interruption, not even SAA passage. At the beginning of each visit a 60 second sub-array exposure was taken to warm up the tungsten lamp. Warming up the lamp prior to data exposures ensures the first exposure and all subsequent exposures will have the expected illumination intensity. The data used in this analysis are summarized in Table 1.

All data were processed through the standard OPUS pipeline and calibrated with CALWFC3 version 2.7 (21-May-2012). The calibration steps included data quality initialization, overscan correction, and subtraction of bias and dark files. In order to achieve the best cosmic ray rejection results, we used a special CRREJTAB file, sky_mean_crr.fits, where SKYSUB = mean, CRRADIUS = 2.1 pixels, CRTHRESH = 0.5555, CRSIGMAS = 6.5, 5.5, 4.5, and SCALENSE = 3.0.

				Chip 1			Chip 2		
Image name	**Obs date**	**Exp time**	**Binning**	**Mean**	**Stdev**	**Median**	**Mean**	**Stdev**	**Median**
ibvh01aqq	12/5/11	30	2	34197	2969	34279	37410	3304	37286
ibvh01apq	12/5/11	30	2	34234	2973	34365	37450	3308	37287
ibvh01aoq	12/5/11	0.5	2	548.2	66.57	550.3	596.9	91.39	594.9
ibvh01anq	12/5/11	0.5	2	548	67.51	550.1	596.7	81.84	595.2
ibvh01amq	12/5/11	17	2	19344	1627	19428	21129	1845	21090
ibvh01alq	12/5/11	17	2	19324	1625	19435	21107	1840	21056
ibvh01akq	12/5/11	6	2	6805	569.6	6847	7420	653.1	7414
ibvh01ajq	12/5/11	6	2	6794	573.9	6833	6408	651.3	7398
ibvh07v9q	12/7/11	5	1	1408	128.6	1415	1533	140.9	1529
ibvh07v8q	12/7/11	5	1	1411	322.6	1416	1534	147.5	1530
ibvh07v6q	12/7/11	12	1	3372	289.4	3391	3672	324.1	3665
ibvh07v5q	12/7/11	12	1	3365	284.8	3382	3663	322.4	3655
ibvh06tgq	12/7/11	1	1	281.6	67.89	282.1	306.6	45.07	305.4
ibvh06tfq	12/7/11	1	1	283	48.98	283.2	307.9	48.19	306.6
ibvh06tdq	12/7/11	45	1	12635	1096	12682	13778	1218	13751

Table 1: *Summary of images used in the Cycle 19 analysis. Unit for statistics is DN, Exposure time is in seconds. Continued on next page.*

				Chip 1			Chip 2		
Image name	**Obs date**	**Exp time**	**Binning**	**Mean**	**Stdev**	**Median**	**Mean**	**Stdev**	**Median**
ibvh06tbq	12/7/11	45	1	12603	1093	12655	13742	1215	13702
ibvh03b7q	12/8/11	13	3	33307	2706	33495	36432	3069	36316
ibvh03b6q	12/8/11	13	3	33317	2706	33491	36442	3070	36391
ibvh03b5q	12/8/11	11	3	28167	2287	28240	30797	2604	30716
ibvh03b4q	12/8/11	11	3	28162	2286	28259	30791	2602	30753
ibvh03b3q	12/8/11	2	3	5105	540	5131	5560	485.2	5553
ibvh03b2q	12/8/11	2	3	5110	422.4	5138	5570	485.9	5565
ibvh03b1q	12/8/11	9	3	22997	1866	23095	25130	2131	25099
ibvh03b0q	12/8/11	9	3	22986	1864	23114	25118	2131	25058
ibvh03azq	12/8/11	0.5	3	1228	151.5	1234	1338	135.8	1335
ibvh03ayq	12/8/11	0.5	3	1228	113.9	1234	1338	134.5	1334
ibvh03axq	12/8/11	3	3	7649	631.9	7689	8340	727.3	8331
ibvh03awq	12/8/11	3	3	7651	623.2	7683	8343	718	8325
ibvh03avq	12/8/11	7	3	17854	1449	17923	19498	1662	19469
ibvh03auq	12/8/11	7	3	17845	1445	17947	19488	1659	19439
ibvh03atq	12/8/11	1	3	2533	228	2547	2760	251.9	2755
ibvh03asq	12/8/11	1	3	2556	398	2568	2783	273.2	2779
ibvh03arq	12/8/11	5	3	12717	1042	12778	13878	1186	13867
ibvh03aqq	12/8/11	5	3	12682	1030	12741	13840	1186	13828
ibvh05l1q	12/9/11	80	1	22465	1925	22575	24526	2145	24460
ibvh05l1q	12/9/11	80	1	22520	1930	22585	24587	2149	24477
ibvh08okq	12/10/11	2	1	564.2	66.34	566.1	613.9	71.17	611.3
ibvh08ojq	12/10/11	2	1	562.2	77.9	564	611.6	71.5	609.5
ibvh08ohq	12/10/11	25	1	7019	593.6	7055	7647	667.4	7634
ibvh08ogq	12/10/11	25	1	7001	590.7	7036	7628	664.8	7611
ibvh04n6q	12/10/11	105	1	29585	2499	29639	32326	2782	32195
ibvh04n5q	12/10/11	105	1	29511	2494	29653	32245	2777	32087
ibvh02moq	12/10/11	24	2	27283	2339	27382	29827	2622	29744
ibvh02mnq	12/10/11	24	2	27261	2337	27403	29801	2615	29756
ibvh02mmq	12/10/11	2	2	2262	248.2	2275	2464	260.8	2460
ibvh02mlq	12/10/11	2	2	2265	218.2	2278	2468	226.5	2465
ibvh02mkq	12/10/11	1	2	1129	126.6	1135	1230	126.3	1228
ibvh02mjq	12/10/11	1	2	1136	108.1	1142	1238	122.1	1236
ibvh02miq	12/10/11	11	2	12442	1036	12498	13578	1186	13559
ibvh02mhq	12/10/11	11	2	12412	1034	12474	13544	1184	13539
ibvh10kfq	6/5/12	80	1	22444	1923	22481	24507	2143	24396
ibvh10keq	6/5/12	80	1	22389	1919	22438	24448	2140	24363
ibvh13o5q	6/8/12	2	1	564.8	57.1	567.2	614.6	71.1	612.5
ibvh13o4q	6/8/12	2	1	563.7	91.63	565.7	613.2	63.34	611.1
ibvh13o2q	6/8/12	25	1	7023	596.2	7055	7652	665.2	7635
ibvh13o1q	6/8/12	25	1	7007	595.3	7041	7635	665.4	7620
ibvh12nyq	6/8/12	5	1	1406	127.4	1414	1531	142.6	1527
ibvh12nxq	6/8/12	5	1	1404	126.4	1411	1529	138.6	1525
ibvh12nvq	6/8/12	12	1	3366	284.6	3384	3665	321.7	3658
ibvh12nuq	6/8/12	12	1	3358	283.8	3377	3657	322.5	3649
ibvh11m8q	6/8/12	1	1	280.6	43.06	280.8	305.2	45	304
ibvh11m7q	6/8/12	1	1	281.5	42.57	281.8	306.2	37.04	305
ibvh11m5q	6/8/12	45	1	12612	1095	12670	13754	1217	13727
ibvh11m3q	6/8/12	45	1	12582	1091	12624	13722	1215	13704
ibvh09d4q	6/11/12	105	1	29492	2493	29560	32229	2777	32118
ibvh09d3q	6/11/12	105	1	29436	2488	29535	32168	2773	31987

Table 1: *Continued.*

3 Method

In accordance to previous WFC3 UVIS gain measurements (Borders 2011, Baggett & Borders 2009, and Baggett 2008) we used the standard mean-variance technique. In order to implement this procedure, we created an average and difference image, for both chips, from a pair of exposures taken in sequence. Before creating the average and difference images the exposures were cleaned of cosmic rays. We flagged the cosmic rays in our data by comparing the data quality extension (DQ, ext3 and ext6 for chips 2 and 1, respectively) with the science extensions (ext1 and ext4 for chips 2 and 1, respectively). In the DQ extension cosmic rays are flagged with value of '8192', our analysis disregards any value other than zero.

The nominal instrument gain was calculated via the mean-variance method, plotting the variance as a function of the mean signal. We used IRAF's tlinear task to fit a linear line to the data, the reciprocal of which is the gain in e-/DN. The tlinear fit is weighted based upon the reciprocal of the standard deviation squared, i.e., more weight on the lower illumination levels. Using IRAF's imstat task, the mean signal was measured on the average images, while the variance (standard deviation squared divided by 2) was measured from the difference images. Statistics were performed on 25 400x400 pixel regions (per quadrant) resulting in Figure 1, where each data point corresponds to a single pixel region. The deviation of higher mean levels from the fit is discussed in our Results. Table 2 summarizes the total gain monitoring results through Cycle 19.

The same mean-variance method was used for the binned data, with the addition of iterative 3σ clipping in the imstat step to mask bad pixels. These bad pixels were due to the influence of bad columns and cosmic rays on the smaller image sections being used, as was seen in the binned data from TV3. The 2x2 binned statistics were computed on 25 200x200 pixel regions, while the 3x3 binned data statistics were computed on 25 133x133 pixel regions, per quadrant. The results of the mean-variance figures for the 2x2 binning are shown in Figure 2, Figure 3 for the 3x3 binning mode, and measurements are summarized in Table 3.

Quadrant	**Cy19**	**Cy 18**	**Cy 17**	**SMOV**	**TV3**
A	1.56	1.55	1.54	1.56	1.56
B	1.56	1.55	1.54	1.56	1.56
C	1.58	1.57	1.56	1.58	1.58
D	1.57	1.56	1.55	1.57	1.57

Table 2: *Gain values for TV3 testing through Cycle 19.*

	2x2 Binning		3x3 Binning	
Quadrant	**Cy 19**	**TV3**	**Cy 19**	**TV3**
A	1.56	1.56	1.55	1.55
B	1.56	1.55	1.54	1.55
C	1.57	1.58	1.56	1.56
D	1.57	1.57	1.56	1.56

Table 3: *Gain values for binned data.*

4 Results and Conclusions

The gain for the nominal setting of 1.5 e-/DN as measured for Cycle 19 unbinned mode are: 1.56, 1.56, 1.58, and 1.57 e-/DN for quadrants A, B, C, and D, respectively. The 2x2 binned mode yielded measurements of: 1.56, 1.56, 1.57, and 1.57 e-/DN, The 3x3 binned mode gain measurements were 1.55, 1.54, 1.56, 1.56 e-/DN for quadrants A, B, C, and D, respectively. Formal errors propagated from the errors of the linear weighted fit are 0.001 e-/DN however, based on gain values obtained using even smaller image subsections, we estimate that the true errors on the gain are higher, $\sim$0.01 e-/DN.

In Figure 1, the mean values show a systematic deviation from the weighted fit at the higher illumination levels which is not evident in the binned modes. Variations in the lamp output or shutter-shading differences could cause such systematics but have been ruled out in this case. As mentioned in the data section, a short sacrificial subarray internal flat field is taken at the beginning of every visit; this ensures the lamp is fully operational and warmed up before the gain exposures are acquired. In addition, comparisons of the illumination levels of pairs of identical full-frame exposures show countrates are stable to «0.5%.

Shutter-shading effects, i.e., differences in effective exposure time due to differences in shutter blade travel time, are expected to be negligible as well. An assessment of shutter behavior after the installation of WFC3 on-orbit found that exposure time variations were <0.0009 sec and no shutter-shading correction is required (Hilbert, 2009). Some systematic differences were seen between commanded and actual exposure durations in early exposures with <1 sec exposure time but the issue has since been fixed. As for shutter repeatability, there was some evidence for a small (1%) effect at the shortest (<1sec) exposure times, which if real, could affect the data but only the lowest exposure level.

Finally, we note that Downing et al. (2006) have reported seeing a non-linear mean variance in similar CCDs on the NTT telescope at La Silla Paranal observatories; they speculate that it may be caused by charge diffusion or migration. Their conclusion is that although it affected their gain value (15%) the signal linearity itself remained excellent and unaffected. Whether this effect may be present in the WFC3 detectors is under investigation.

The goal of the current analysis has been to evaluate the gain in order to monitor for any relative changes over time. Using the same technique as during previous cycles, we find the gain has remained constant to within 1-2% of previously calculated values.

References

Baggett, S., WFC3 ISR 2008-12, "WFC3 TV3 Testing: UVIS Channel Calibration Subsystem Performance"

Baggett, S., WFC3 ISR 2008-13, "WFC3 TV3 Testing: UVIS-1 Gain Results"

Baggett, S. and T. Borders, WFC3 ISR 2009-29, "WFC3 SMOV Proposal 11419: UVIS Gain"

Borders, T., C. Pavlovsky, S. Baggett, WFC3 ISR 2011-13, "WFC3 Cycle 17 Proposal 11906: UVIS Gain"

Downing, M. et al., Proc. SPIE 6276, 627609 (2006)

Dressel, L., 2012. "Wide Field Camera 3 Instrument Handbook, Version 5.0"

Hilbert, B., WFC3 ISR 2009-25, "WFC3 SMOV Program 11427: UVIS Channel Shutter Shading,"

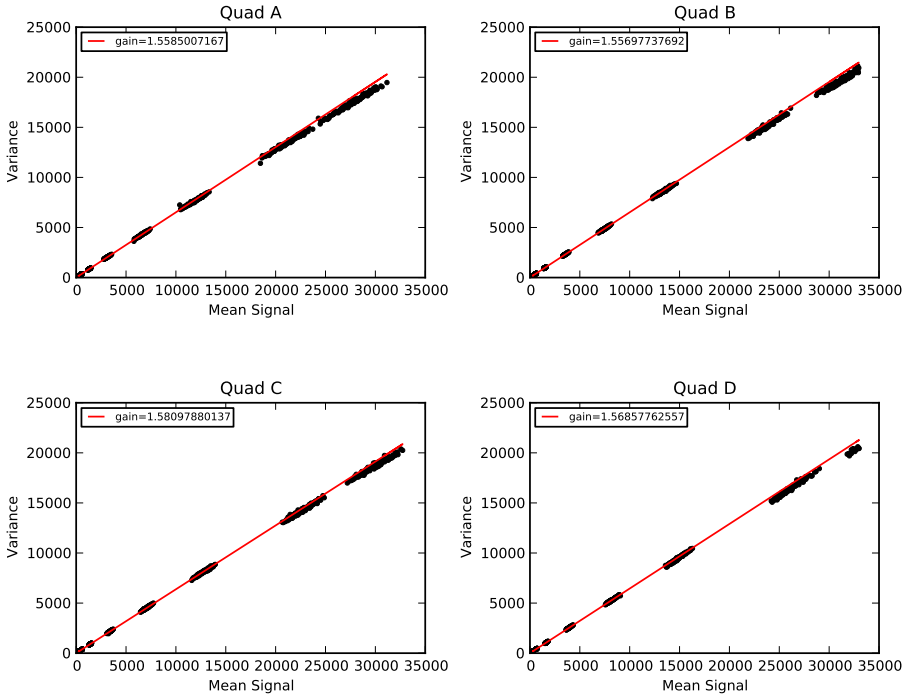

Figure 1: *Variance as a function of the Mean for the unbinned Cycle 19 data.*

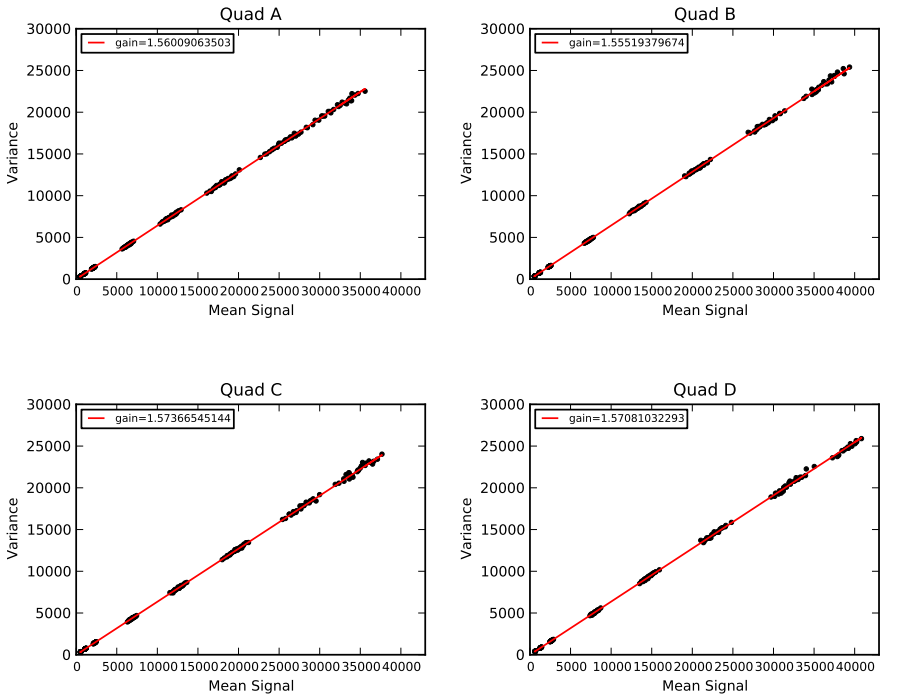

Figure 2: *Variance as a function of the Mean for the 2x2 binned Cycle 19 data.*

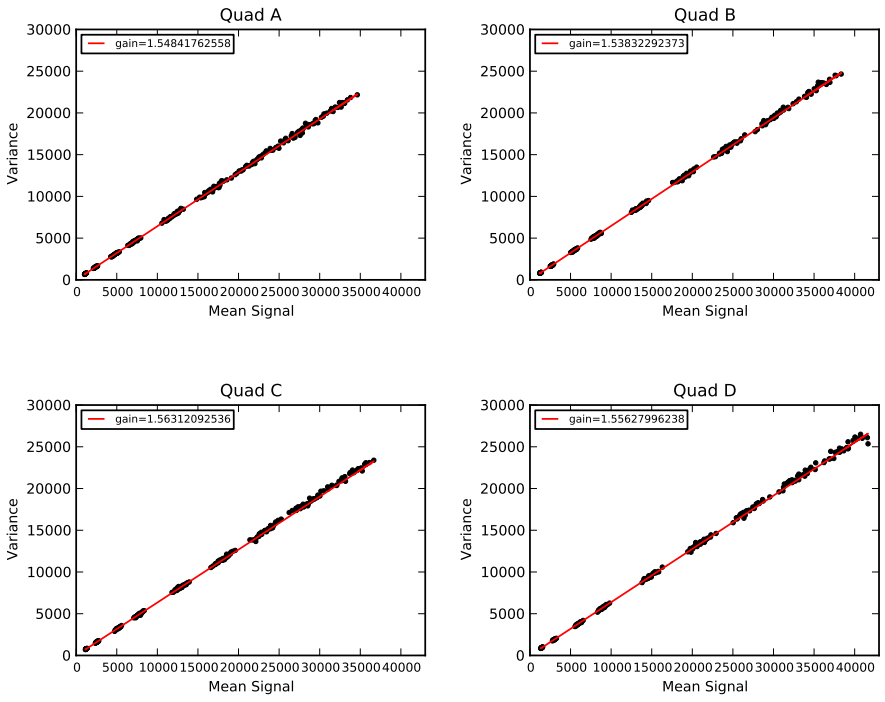

Figure 3: *Variance as a function of the Mean for the 3x3 binned Cycle 19 data.*